Characterization of Sputtered BZT Thin Films for MCM: Multichip Module

Nobuo Kamehara, Mineharu Tsukada, Jeffrey S. Cross, and Kazuaki Kurihara
Fujitsu Laboratories Ltd., Atsugi 243-01, Japan

$Ba(Zr, Ti)O_3$ [BZT] thin films were prepared for potential use as a decoupling capacitor for a multichip module (MCM). The crystal structure of BZT thin films on Pt(100)/MgO(100) and MgO(100) deposited from $Ba(Zr_{0.2}Ti_{0.8})O_3$ powder targets has a perovskite structure and is strongly (100) oriented. The crystal structure of BZT thin films on Pt(111) coated substrates differ from that of Pt(100)/MgO(100) and MgO(100) substrates. The degree of preferred (100) orientation on $Pt(111)/SiO_2/Si$ increased with increasing deposition temperature. We obtained a maximum dielectric constant of 150 at 600°C deposition. The loss tangent, leakage current and temperature dependence of capacitance of these BZT thin films were very small.

Introduction

Generally, chip capacitors and multilayer chip capacitors (MLCs) are used for multichip modules (MCMs) since they have high reliability, large capacitance, and are compatible with present operating frequencies. However, the clock frequencies being used with MCMs continue to increase (Figure 1). In order to produce a higher performance, higher speed MCM, there is a great need for lower inductance decoupling capacitors to reduce switching noise at high frequencies (Dey and Lee, 1992). Chip capacitors have a limited frequency range because of their lead inductance. In particular, they don't work well for clock frequencies above 100 MHz. Therefore, we must consider using a capacitor which is in the LSI chip or the MCM. The use of a thin film decoupling capacitor on the MCM substrate promises high performance at a high frequency due to its low inductance. The use of thin film capacitors incorporated into the MCM will replace MLC mounted on the MCM surface. As a result, more LSI chips can be mounted on the MCM surface.

One such perovskite ferroelectric ceramics material BZT $[Ba(Zr,Ti)O_3]$ has excellent bulk properties for meeting the anticipated need for a high dielectric material. Its bulk dielectric constants is greater than 20,000 (Sakai Chemical). However, to our knowledge, limited thin film research has been published on the preparation and characterization of this material. In this study, we deposited BZT thin films by a sputtering method and investigated the effect of the substrates and deposition temperature on the dielectric properties for potential use as a decoupling capacitor.

Experimental Studies

BZT $[Ba(Zr,Ti)O_3]$ thin films from a single target system were sputtered using BZT powder containing 20 mol % of Zr. BZT thin films were deposited on MgO(100) substrates, Pt(111)/MgO(100) substrates, Pt(100)/MgO(100) substrates, and $Pt(111)/SiO_2/Si$ substrates. The sputtering gas pressure was 1 Pa and $Ar:O_2$ gas ratio of 9:1 was used. The deposition temperature was 450–600°C for 5 h. The input rf power was 1.6 W/cm^2.

A 100-nm-thick sputtered Pt film was deposited as the bottom electrode and was used in order to measure electrical

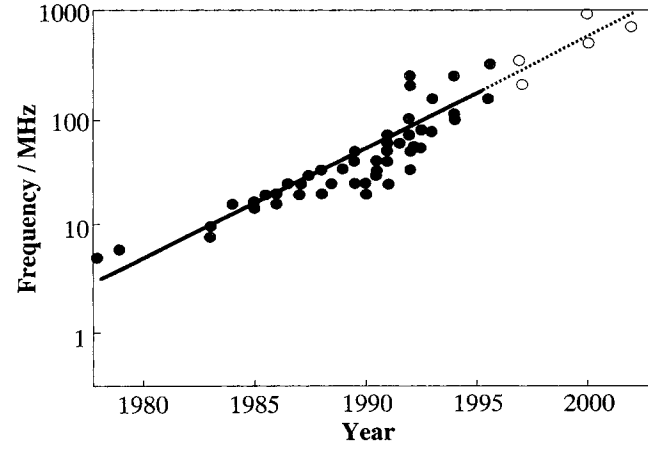

Figure 1. Clock frequency of MCM.

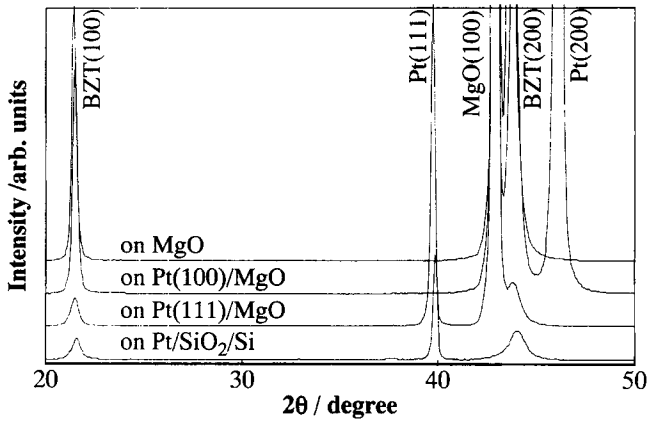

Figure 2. XRD patterns of BZT thin films on various substrates.

properties of the BZT. According to XRD measurements, the Pt deposited at room temperature on MgO (100) substrates had a (111) orientation and a (100) orientation when deposited at 500-600°C on MgO(100) substrates.

We analyzed the crystal structure by XRD, and the microstructure and thickness by FE-SEM and TEM. Electrical properties such as the dielectric constant, loss tangent, temperature dependence of capacitance, and leakage current were measured using an impedance analyzer and picoampere meter.

Results

A BZT thin film deposited on Pt(100)/MgO(100) and MgO(100) by sputtering from $Ba(Zr_{0.2}Ti_{0.8})O_3$ powder targets has a perovskite crystal structure and is strongly (100) oriented as indicated by XRD patterns as shown in Figure 2. The BZT thin film on Pt(111)/SiO_2/Si and Pt(111)/MgO(100) substrate has also a perovskite structure. However, the XRD peak intensity of BZT(100) is weak compared with that on Pt(100)/MgO(100) and MgO(100). Figure 3 shows the influence of the deposition temperature on the Pt(111)/SiO_2/Si substrate. The crystallinity based on XRD peak intensity increases with deposition temperature.

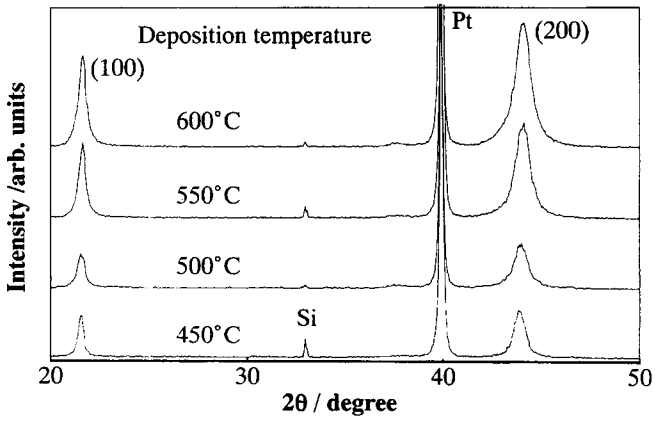

Figure 3. XRD patterns of BZT thin films on Pt(111)/SiO_2/Si substrate at various deposition temperatures.

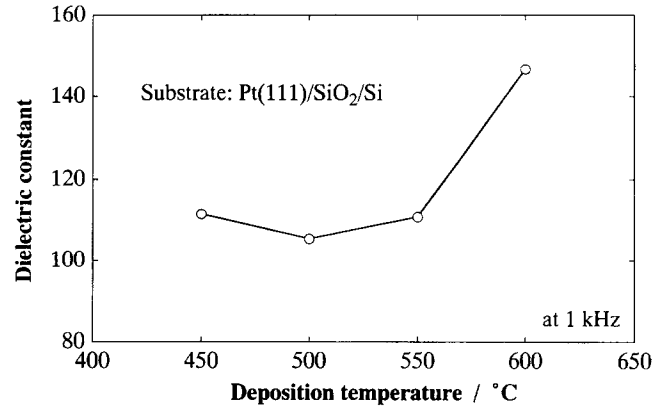

Figure 4. Dielectric constant vs. deposition temperature.

The relationship between the dielectric constant and the loss tangent measured at 1 kHz on the Pt(111)/SiO_2/Si substrate and the deposition temperature of a BZT film is shown in Figures 4 and 5. The film thicknesses are approximately 500 nm based on FE-SEM photographs. Both the dielectric constant and the loss tangent increase slightly with increasing deposition temperature. The maximum dielectric constant measured was about 150. The dielectric constant on the Pt(100)/MgO(100) and MgO(100) is also between 100 to 150 for deposition temperatures between 450 and 600°C. There is almost no influence of the substrates on the film dielectric properties.

The temperature dependencies of capacitance for the various substrates are shown in Figure 6. The capacitance change from −35 to 125°C compared to that at room temperature is less than ±2%. The capacitance of the film on the SiO_2/Si substrate monotonously increases with the temperature, but decreases on the MgO substrate. These results indicate that the temperature dependence of capacitance is influenced mainly by the choice of substrate material and is influenced the crystallinity of the thin film. The change in capacitance with temperature appears to be caused by the thermal expansion difference between the thin film and the substrate.

The temperature dependencies of the loss tangent for various substrates are shown in Figure 7. The change in the loss tangent from −35 to 125°C in comparison to that of room

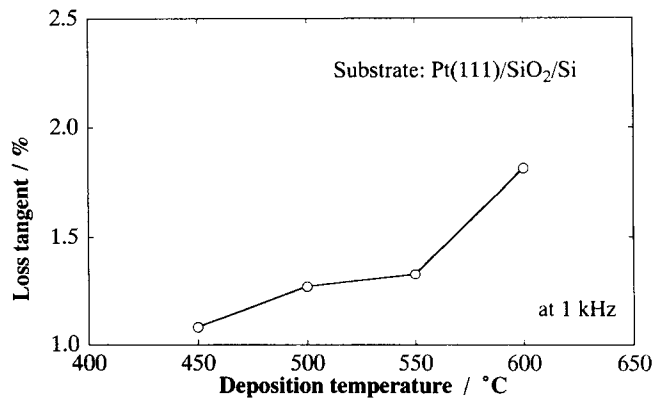

Figure 5. Loss tangent vs. deposition temperature.

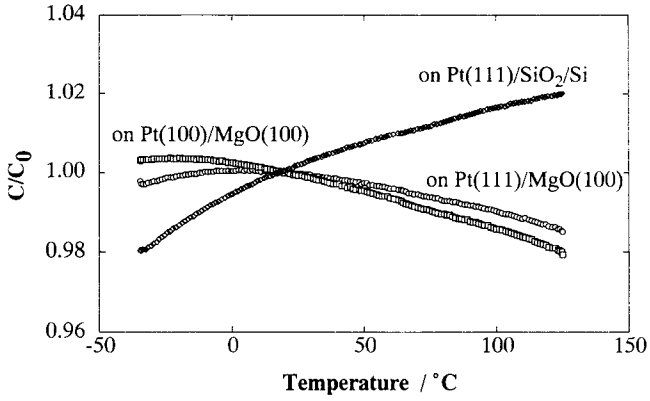

Figure 6. Temperature dependence of capacitance of BZT thin films on various substrate.

C_o is capacitance at 20°C.

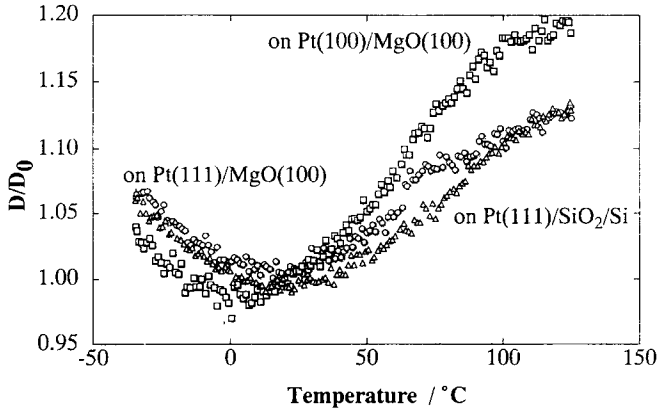

Figure 7. Temperature dependence of loss tangent of BZT thin films.

D_o is loss tangent at 20°C.

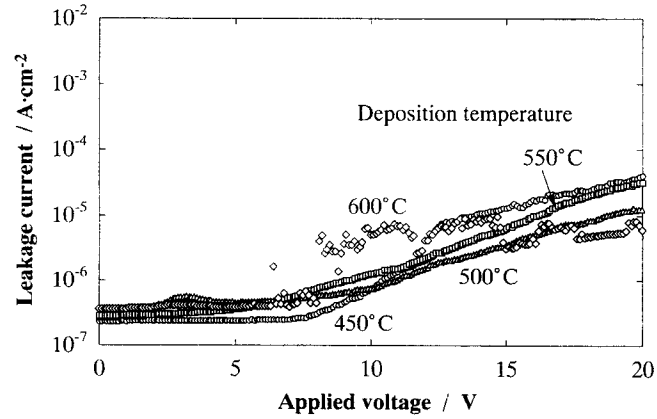

Figure 8. Relationship between leakage current of BZT thin films on Pt(111)/SiO_2/Si and applied voltage.

temperature is less than ±10% for the 600°C deposited film. The relationship between the leakage current of BZT thin film deposited on the Pt(111)/SiO_2/Si substrate is shown in Figure 8. The leakage current is constant until about 7 V and then the leakage current increases with applied voltage. The deposition temperature seems to have little effect on the leakage current.

The microstructure of BZT thin films on different substrates is shown in Figure 9. The thickness of both films is about 500 nm. However, their XRD crystallographic orientation varies with the substrates, yet, the structure of the film is almost same. The grain size of both films is very small, it is less than 50 nm as shown in Figure 9.

High resolution TEM micrographs show a 10-nm-thick interfacial layer between the Pt electrode and the BZT thin film as shown in Figure 10. Moire patterns in the BZT thin films are also observed, and the crystal size is about 25 nm.

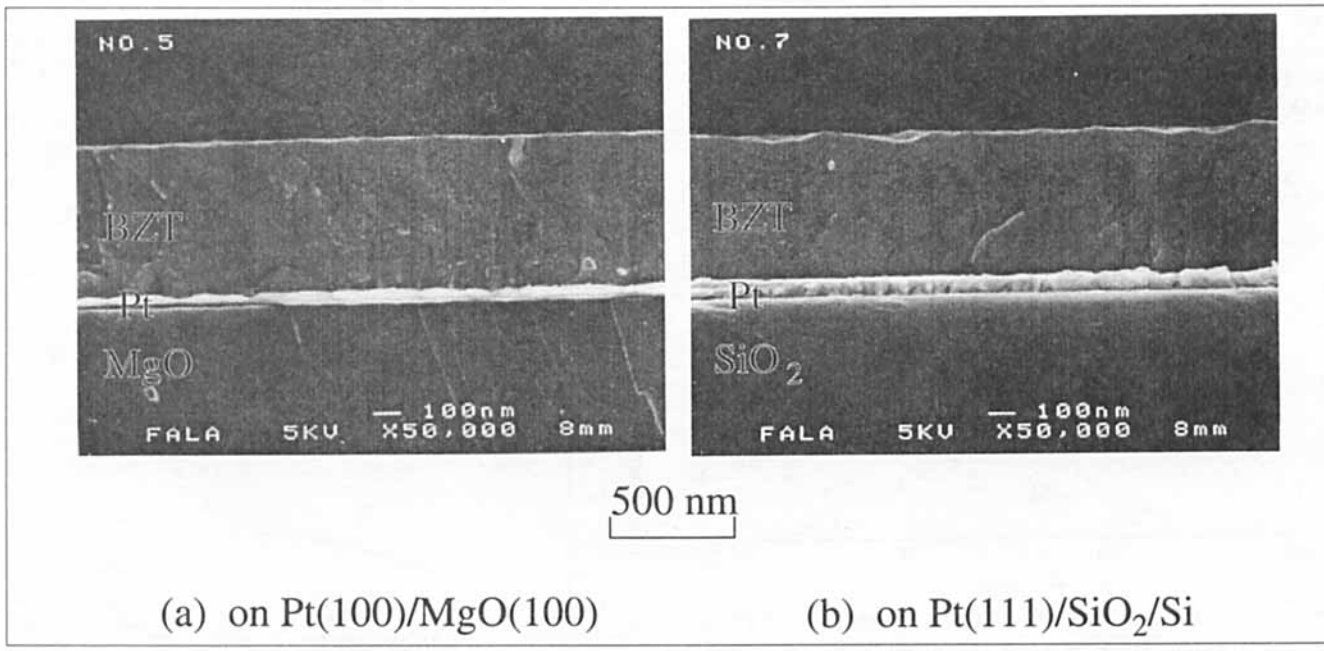

Figure 9. SEM cross section of thin films of (a) BZT/ Pt(100)/MgO(100); (b) BZT/Pt(111)/SiO_2/Si.

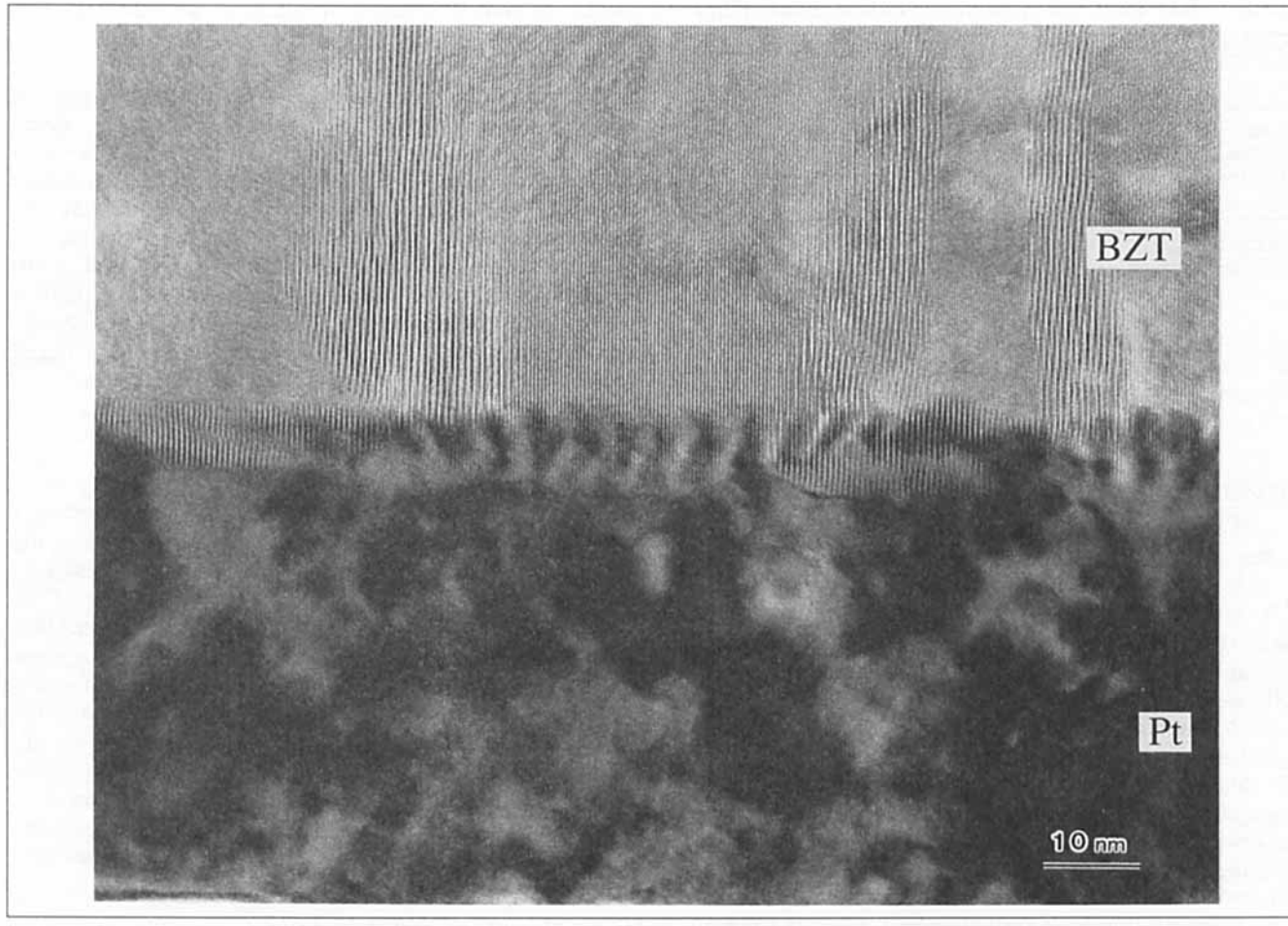

Figure 10. Cross-sectional TEM image of interface between BZT thin film and Pt electrode.

The BZT thin film showed epitaxial-like grain growth where the crystalline lattice planes are normal to the interface, although the width of the Pt and BZT planes are different. The lattice constants of Pt and BZT reported in the literature are 3.92 A (face-center cubic structure) and about 4.04 A (perovskite structure), respectively. Figure 11 shows electron diffraction patterns of BZT thin films. Based upon the electron diffraction patterns of the Pt electrode and BZT thin film, these materials are clearly crystalline.

The electrical properties of a BZT thin film and conventional bulk BZT are shown in Table 1. The thin film dielectric constant reaches about 150, which is quite small compared with the bulk BZT. However, this value may be enough for use as a thin film decoupling capacitor in an MCM. The

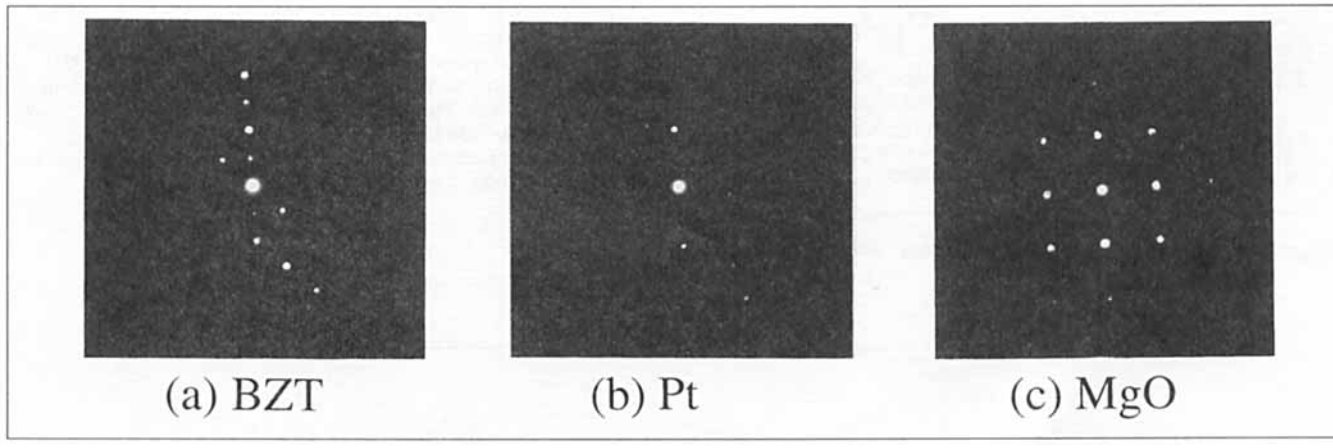

Figure 11. Electron diffraction patterns of BZT/Pt/MgO thin films.

Table 1. BZT Electrical Properties of Bulk and Thin Films

Properties	Specification	Bulk BZT*	Our Study
Dielectric const.	100 ~ 1,000	6,900	~ 150
Loss tangent (%)	< 3.0	0.6	1.1 ~ 2.3
Temp. dependence (%)	−56 ~ +22	> 300	< ±2
Leakage current (A/cm^{-2})	$\leq 10^{-6}$	—	$\leq 10^{-6}$
High freq. properties	Excellent	—	?
Effect of heat treatment**	Stable	—	?

* $Ba(Zr_{0.2}Ti_{0.8})O_3$.
** Curing process of polyimide.

thin film loss tangent is less than 3%, and this may be useful for reducing ECR at high frequencies. The temperature dependence of thin film capacitance is less than 2% between −35 and +125°C, which meets the Z5U specification.

Discussion

At this time, we are not aware of any other studies on the sputter deposition of BZT films, and, therefore, further comparisons with published data is not possible. However, if these BZT results are compared to a similar material such as $(Ba,Sr)TiO_3$ thin films, relationships between process conditions and dielectric properties can be elucidated.

It has been shown previously with BST films that the deposition temperature strongly influences the film grain size, crystallinity, and dielectric constant (Kuroiwa et al., 1994). BST films deposited at temperatures of 660 and 750°C had larger grain sizes and higher dielectric constants compared to films deposited at less than 600°C. In the present study with BZT the deposition temperature was 600°C or less resulting in films with small grains as seen in Figures 9 and 10.

In a separate deposition study of BST films, the film dielectric constant was shown to be strongly related to film thickness (Gitel'son et al., 1977). With film thicknesses of less than 1,000 nm, a curie temperature as noted by a maximum in the dielectric constant as a function of temperature was not observed due to internal film stress. These results are similar to what is observed in this study with BZT films as shown by the relatively flat capacitance vs. temperature relations observed in Figure 6.

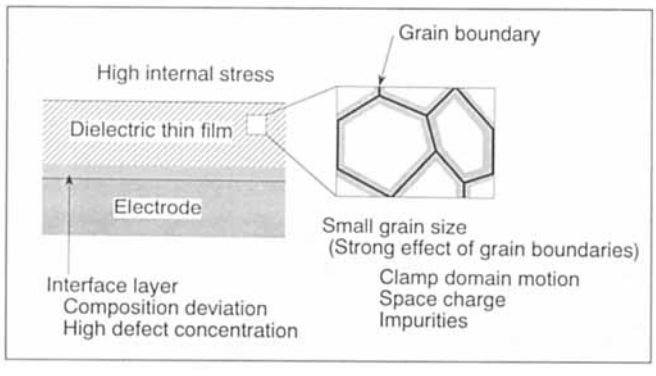

Figure 12. Possible reasons for low dielectric constants in thin films.

The relationship between the film dielectric properties and physical properties are summarized in Figure 12. As noted above, the BZT films have a relatively small grain size which reduces domain motion. Internal film stress and crystalline defects in the film which develop when cooling down the film from the deposition temperature to room temperature are yet other reasons (Gitel'son et al., 1977; Rossetti et al., 1991; Funakubo et al., 1995). Further research is needed particularly at higher deposition temperatures to clarify the relationship between the BZT film dielectric properties and physical properties.

Conclusion

BZT thin films were deposited by sputtering from $Ba(Zr_{0.2}Ti_{0.8})O_3$ powder targets. The crystal structure of BZT thin films has a perovskite structure. The orientation of the film is strongly influenced by the substrates and show preferred (100) orientation on Pt(100)/MgO(100) and MgO(100) substrates. The degree of (100) orientation on Pt(111)/SiO_2/Si increased with deposition temperature. The maximum dielectric constant we measured was about 150 with a deposition temperature of 600°C. The loss tangent and the leakage current of these BZT thin films was small. The dielectric constants of the BZT films deposited in this study were much lower than that of bulk BZT ceramics. However, the thickness of the thin film capacitor is less than one-tenth of a chip capacitor, so it may have a large enough dielectric constant for MCM usage.

Literature Cited

Dey, S. K., and J. J. Lee, "Cubic Paraelectric (Nonferroelectric) Perovskite PLT Thin Films with High Permittivity for ULSI DRAM's and Decoupling Capacitors," *IEEE Trans. on Electron Devices*, **39,** 1607 (1992).

Funakubo, H., M. Otsu, Y. Inagaki, K. Shinozaki, and N. Mizutani, "General Rule for the Determination of c-axis Orientation of Pb-Based Tetragonal Ferroelectric Oxide Film Prepared by CVD," *J. Mat. Sci. Let.*, **14,** 629 (1995).

Gitel'son, A. A., A. M. Lerer, V. S. Mikhalevskii, V. M. Mukhortov, and S. V. Oriov, "Physical Properties of $(Ba,Sr)TiO_3$ Ferroelectric Thin Films in Weak Electric Fields," *Sov. Phys. Solid State*, **19,** 1121 (1977).

Kuroiwa, T., Y. Tsunemine, T. Horikawa, T. Makita, J. Tanimura, N. Mikami, and K. Sato, "Dielectric Properties of $(Ba_xSr_{1-x})TiO_3$ Thin Films Prepared by RF Sputtering for Dynamic Random Access Memory Application," *Jpn. J. Appl. Phys.*, **33,** 5187 (1994).

Rossetti, G. A. Jr., L. E. Cross, and K. Kushida, "Stress Induced Shift of the Curie Point in Epitaxial $PbTiO_3$ Thin Films," *Appl. Phys. Lett.*, **59,** 2524 (1991).

"Perovskite Compounds," Technical Datasheets, Sakai Chemical Industry Co., Osaka, Japan.

Manuscript received Oct. 28, 1996, and revision received May 13, 1997.